

Fast Combined Separability Filter for Detecting Circular Objects

Yasuhiro Ohkawa Chendra Hadi Suryanto Kazuhiro Fukui
Graduate School of Systems and Information Engineering,
University of Tsukuba, Japan
{ohkawa@cvlab.cs, chendra@cvlab.cs, kfukui@cs}.tsukuba.ac.jp

Abstract

In this paper, we propose a fast combined separability filter, which can selectively detect circular features such as pupils and nostrils in an image of the human face. The proposed filter is designed as a combination of multiple rectangle separability filters so that it can achieve high-speed processing and high positioning accuracy at the same time. The evaluation experiments using synthetic images and real face images show that the proposed filter is 70 times faster than the conventional circular separability filter.

1 Introduction

Detecting feature points from an input image is a fundamental process in computer vision. The accuracy of detecting feature points largely affects the total performance of a recognition system, especially as the positions of the feature points are used in the object segmentation process before performing the recognition process.

There have been various types of filters for extracting feature points. In particular, the circular separability filter [3] is one of the most effective filters and has been widely used for various applications, such as detection of pupils and nostrils [3, 7, 10], tracking of human head [6], a ball in a soccer broadcast [9] and moving particles on an axon in medical image [4].

The circular separability filter (CSF) is an extension of the rectangle separability filter [2]. It is a region-based filter with a very good capability for extracting low contrast step and line edges. The rectangle separability filter (RSF) consists of multiple regions. In the simplest configuration for extracting step edges, the rectangle separability filter consists of two rectangle regions (RSF2), and outputs the separability between distributions of image intensities of the two regions, where the separability is calculated according to the Fisher criterion. The rectangle separability filter with three regions (RSF3) can extract line and roof edges. In CSF, the two rectangle regions of RSF2 are replaced with two concentric ring regions. As a result, CSF can extract the radius and center positions of circular feature points.

CSF can detect feature points from a low contrast image even under very noisy conditions. Its positioning accuracy is very high in comparison with gradient-based filters. However, CSF has a serious problem relating to computational complexity, which is derived from the calculations of means and variances of image intensities to obtain the separability map.

Such computational complexity leads to severe difficulty in the real-time execution of multiple-scale CSF. In conventional methods, in order to reduce the computational cost, the separability filter is applied to limited

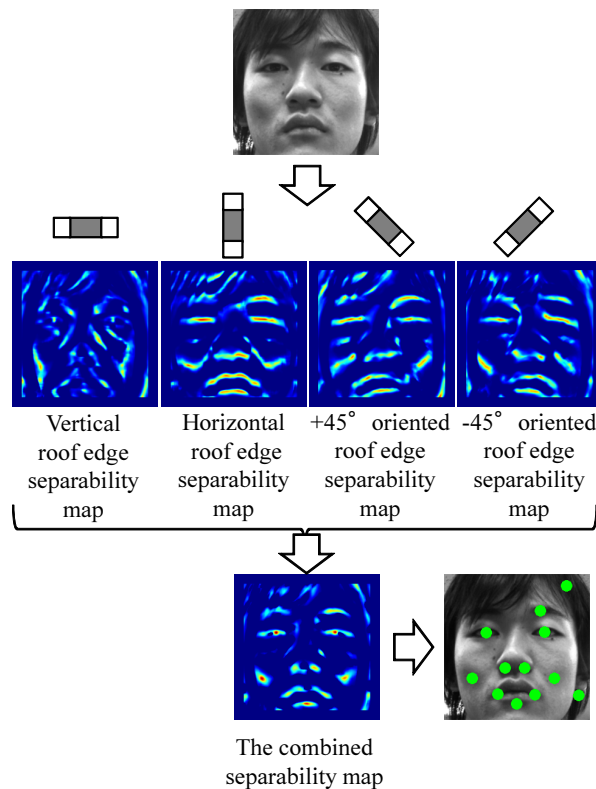


Figure 1. Concept diagram of fast combined separability filter.

regions only, which satisfies some conditions. For example, in the system of face recognition [10], CSF was applied to only the dark regions extracted by using the P-Tile method. However, even if this pre-processing is applied, the computational complexity is still too high to achieve real-time processing of a large image with multiple scales.

To solve this problem, the square separability filter (SSF) has been proposed [8]. The SSF utilizes two concentric square regions instead of two concentric ring regions. The SSF is very fast because the value of separability can be calculated at high speed by using an integral image [5]. However, its positioning accuracy is insufficient because the SSF extracts many other feature points besides those of the pupils and nostrils. This over detection leads to an extra computational cost for verifying whether the extracted candidate is a pupil or nostril by using pattern matching.

To reduce the high computational cost of CSF while retaining its high accuracy and robust performance, we propose a new type of separability filter, which is a combination of multiple rectangle separability filters (RSF3). A typical combination consists of a vertical RSF3, a horizontal RSF3 and ± 45 degree RSF3s as shown in Fig. 1. The output of the proposed filter is

obtained as either an arithmetic or geometrical mean of all the outputs from the RSFs. A single RSF cannot selectively extract a circular feature point, though it can deal with a specific directional line edge. However, the combination of RSFs enables the proposed filter to selectively extract only circular feature points without detecting extra non-circular feature points.

This paper is organized as follows. In Section 2, we describe a separability filter and explain its functions. In Section 3, we explain the process flow of the proposed method. In Section 4, the effectiveness of our method is demonstrated through evaluation experiments with both synthetic images and real face images. Section 5 concludes.

2 Feature Point Detection based on Separability Filter

CSF computes the separability η of two regions of an image as shown in Fig. 2(a) by employing Fisher discriminant analysis. The separability η ($0.0 \leq \eta \leq 1.0$) of two regions R1 and R2 in an image is calculated as the ratio of total variance σ_T^2 and between-class variance σ_b^2 defined by the following equations.

$$\eta = \frac{\sigma_b^2}{\sigma_T^2}, \quad (1)$$

$$\sigma_b^2 = \frac{N_1}{N}(\bar{P}_1 - \bar{P})^2 + \frac{N_2}{N}(\bar{P}_2 - \bar{P})^2, \quad (2)$$

$$\begin{aligned} \sigma_T^2 &= \frac{1}{N} \sum_{P_i \in (R1 \cup R2)} (P_i - \bar{P})^2 \\ &= \bar{P}^2 - (\bar{P})^2, \end{aligned} \quad (3)$$

where N_1 and N_2 are the number of pixels in R1 and R2, respectively, N is the total number of pixels of both regions, P_i is the image feature at pixel i , \bar{P}_1 and \bar{P}_2 are the mean values of the image feature R1 and R2, \bar{P} and \bar{P}^2 are the mean value and the mean square of the image feature from both regions. In the case of $\bar{P}_1 \geq \bar{P}_2$, η is set to 0. By performing CSF on the whole image, we can obtain a separability map in which the local maximum points are considered as the center points of circular objects.

3 The Proposed Separability Filter

3.1 Combination of Multiple Separability Filters

The proposed filter detects circular objects by integrating the outputs of four types of filters as shown in Fig. 2(c-1)~(c-4).

The shape of objects can be estimated based on the distributions of the separability values obtained from each of the four filters. A target object is regarded as a circular object in the case that all of the separability values are large. On the other hand, when all of the separability values are small, we can presume that there is no object. In another cases, the target is regarded as a kind of shape other than a circle.

We define two kinds of outputs for the proposed filter. One is an arithmetic mean of the four outputs: $\mu_A = \frac{1}{n} \sum_{i=1}^n \eta_i$ and the other is a geometric mean μ_G of the four outputs: $\mu_G = \sqrt[n]{\prod_{i=1}^n \eta_i}$. In the case of using the geometric mean, we can ensure that the combined value μ_G is large only if all η_i are large.

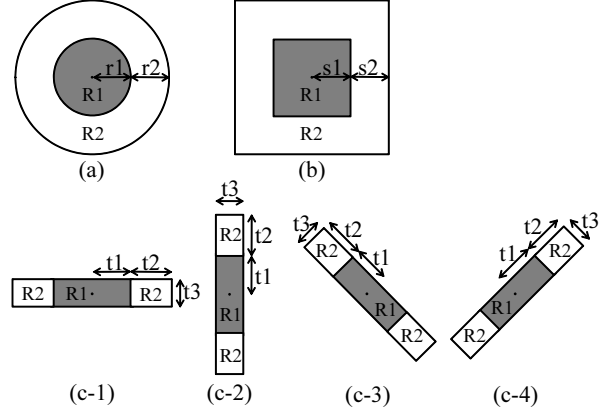


Figure 2. (a) CSF, (b) SSF, (c-1)~(c-4) Component filters (RSF3s) of the proposed separability filter.

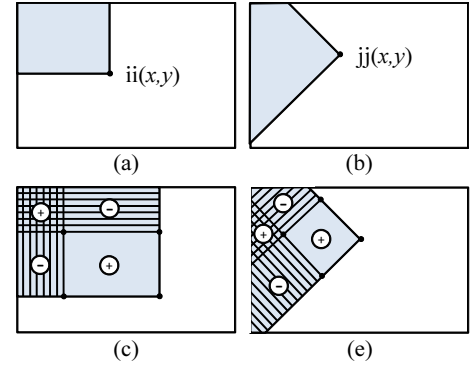


Figure 3. Integral Images: (a) Upright integral image and (b) Rotated integral image; (c) Calculation scheme of a particular integral image region; and (d) Calculation scheme of a particular rotated integral image region.

3.2 Fast Computation of Separability using Integral Image

We have introduced the calculation method of the separability value (Eq.(1)) by using the mean values \bar{P}_1 , \bar{P}_2 , \bar{P} , and the mean square \bar{P}^2 . In this section, we will introduce the concept of the integral image [5] in which we can perform fast computation of the separability values.

The integral image $ii(x,y)$ at coordinate (x,y) of image i is defined as the sum of the pixel values above and to the left of the coordinate (x,y) , as shown in Fig. 3(a) and the following Eq. (4).

$$ii(x,y) = \sum_{\hat{x}=1}^x \sum_{\hat{y}=1}^y i(\hat{x}, \hat{y}), \quad (4)$$

where $i(\hat{x}, \hat{y})$ is an image intensity value at coordinate (\hat{x}, \hat{y}) .

Figure 3(c) shows how to compute the integral image of a particular rectangular region by using four region references. By adopting a similar concept, we can also compute the integral image of a 45° oriented rectangle

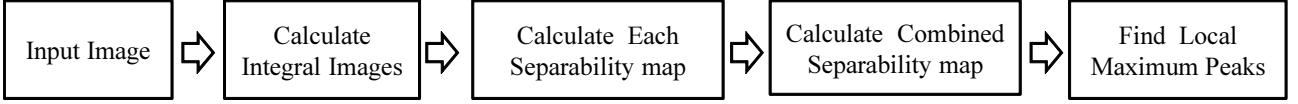


Figure 4. Process flow of detecting circular feature points using the proposed filter.

region as shown in Fig. 3(b) and (d). To calculate the mean square $\overline{P^2}$, firstly we compute P^2 from an input image. Next, we construct the integral image and finally find $\overline{P^2}$.

3.3 Algorithm for Detecting Circular Feature Points

Figure 4 shows the process flow of detecting circular feature points using the proposed filter. The parameters $t1(i)$, $t2(i)$ and $t3(i)$ ($i = 1 \sim N$) are set in advance.

0. Initialization: $i = 1$.
1. Calculate the integral images from an input image.
2. Generate four types of separability maps by using the filter with the parameters $t1(i)$, $t2(i)$ and $t3(i)$ from the integral images.
3. Calculate the arithmetic or geometric mean of all the maps as a new combined separability map.
4. Update: $i = i + 1$, and if $i \leq N$ then go back to step 1, otherwise, go to the next step.
5. For each point, the maximum separability of the N separability maps is set as its value.
6. Find local maximum points from the above separability map as the center position of circular feature points.

4 Evaluation Experiments

We compared the computational complexities and the performances of the CSF (Fig. 2(a)), SSF (Fig. 2(b)), and the proposed filter. Each filter has several parameters for region setting the filter regions as shown in Fig. 2. However, to simplify the control of the region setting, we introduce one parameter, r , so that the parameters $r1, r2, s1$ and $s2$ of CSF and SSF are set to r . The parameters of the proposed filter, $t1$ and $t2$, are also set to r , and $t3$ is set to $\frac{r}{3}$ (round off).

4.1 Evaluation of Computational Complexity

We evaluated the processing time of the conventional filters and the proposed filter in term of the size of the input image and the filters.

The aim of this experiment is to evaluate the processing time. Thus, we used several simple synthetic square images, which have a uniform image intensity with Gaussian noise (SNR=1.0), as input images. The size of the image was changed from 100×100 pixels to 1000×1000 pixels in increments of 100 pixels.

Figure 5 shows the processing time of each filter. In this figure, the horizontal axis denotes the size of the

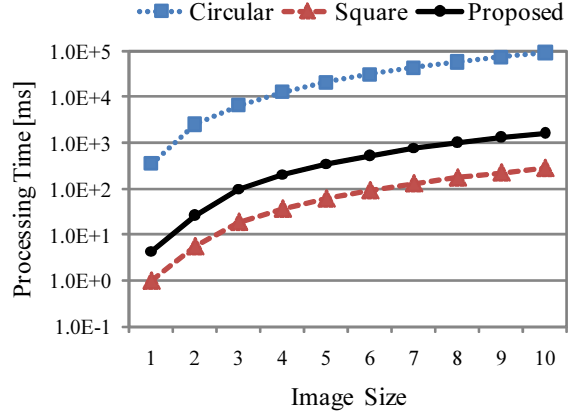


Figure 5. Processing time vs. image size.

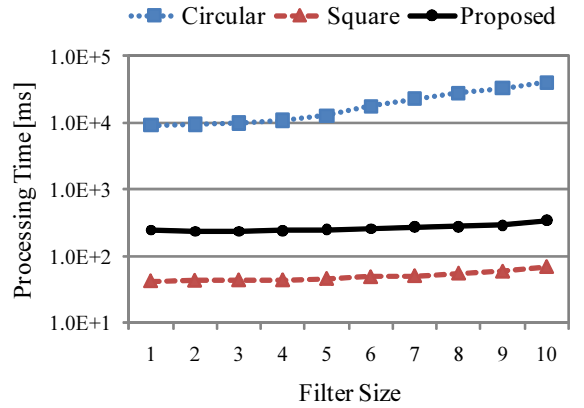


Figure 6. Processing time vs. filter size.

input image and the vertical axis denotes the processing time (ms) on a logarithmic scale.

We can see that the processing time of the proposed filter is much faster than the conventional circular separability filter (CSF). For instance, when applied to an image with a size of 1000×1000 pixels, the processing time of CSF and the proposed filter were 9.2×10^4 ms and 1.65×10^2 ms respectively. In this case, the proposed filter is about 65 times faster than CSF. This fast processing speed will be practical for various applications that require real-time performance.

We can also see that the square separability filter (SSF) is faster than the proposed filter. However, the proposed filter remains useful from a general viewpoint, since the detection performance of SSF is poor compared with the proposed filter, as will be shown later.

Next, we evaluated the changes of the processing

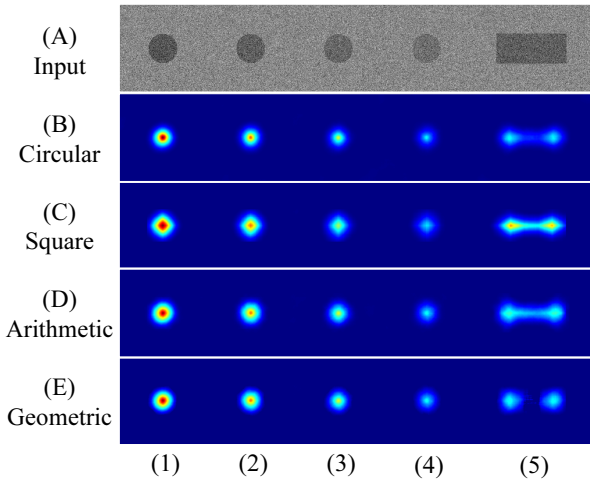


Figure 7. (A) Input image, (B) Circular Separability map, (C) Square Separability map, (D) Combined Separability map (Arithmetic mean), (E) Combined Separability map (Geometric mean), Left to right: (1)SNR = 2.00, (2)SNR = 1.39, (3)SNR = 0.89, (4)SNR = 0.50, (5)SNR = 1.39.

time in terms of the filter size. In this experiment, the size of an input image was fixed to 400×400 pixels, while the filter size was changed. Fig. 6 shows the processing times of all the filters. The result shows that the filter size significantly affects the processing time of CSF. In contrast, the processing times of SSF and the proposed filter are only slightly affected by the change in filter size, in which the processing time of the proposed filter is 70 times faster than that of the CSF.

4.2 Evaluation of Feature Point Detections

In this experiment, we compared the robustness of all the filters against noise, using a synthetic image shown in Fig. 7(A). This image includes four circular objects with a radius of 25 pixels and a rectangle object with a size of 120×50 pixels. Noise of different levels was added to each object. The SNRs of the added noise were 2.00, 1.39, 0.89, 0.50 and 1.39 for (1)~(5), respectively.

Figure 7(B)~(E) shows the separability map of each filter. We can see that the local maximum point detected by each filter corresponds accurately to the center of each circular object without being influenced by the added noise. However, the output of the square separability filter is blurred as a rectangular region, although that of the other filters are sharp.

When applied to a rectangular object, each filter outputs different characteristics of the separability maps as shown in Fig. 7(5). The output of the local maximum from the proposed filter using the geometric mean is relatively low compared with that of the other filters. The proposed method using the arithmetic mean, CSF, and SSF outputs many improper positions of high local maximum points such as at the center lines of the rectangular object.

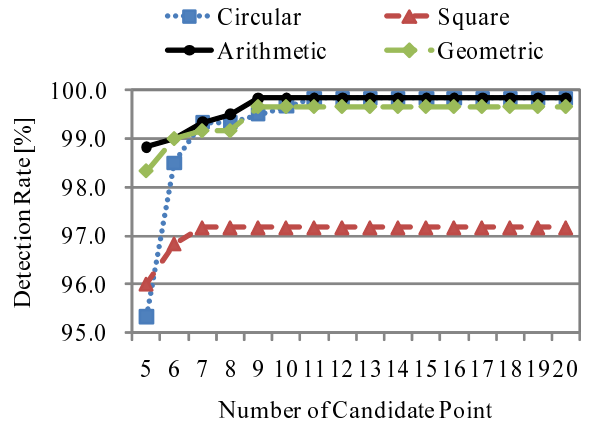


Figure 8. Relationship between the number of local maximum points and detection rate.

4.3 Evaluation of Pupil Detection

We evaluated the effectiveness of the proposed filters in the task of detecting pupils in a face image. The performance was measured in terms of detection rate and positioning error, where the positioning error was defined based on the distance between a specified correct position of a pupil and a detected local maximum point.

We collected 300 face images from three subjects and cropped face regions from them by using the face detection function of OpenCV[1]. The size of the cropped face images was 240×240 pixels as shown in Fig. 9. By this normalization, we could estimate that the radius of the pupil was nearly 8 pixels. Thus, the common parameter r for all the filters was set to 8 pixels. Prior to the experiment, we manually specified the center coordinates of pupils in all images.

In this task, we have to select the correct pupils from many of the largest local maximum points extracted from the separability map. Thus, the number of the local points should be as small as possible since the computational complexity depends on their number.

We consider that a pupil is detected correctly when the distance between the local maximum point and the specified true position is within 4 pixels as shown in Fig. 10. Figure 8 shows the relationship between the number N of the largest local maximum points and the detection rate. We can see that the proposed filter has a comparable performance to that of the CSF. In contrast, the performance of SSF is low.

Table 1 shows the average of positioning errors of all filters. This shows that the proposed filters also outperform the SSF in terms of positioning error. We can conclude the advantage of the proposed filter against CSF by considering the extremely fast processing speed compared to CSF, although the positioning accuracy of the proposed filter is slightly inferior to CSF.

Another observation is that the filter using the arithmetic mean is slightly better than that using the geometric mean. This is because the shape of an eye is often not precisely circle but oval or rectangle due to occlusion by an eyelid.

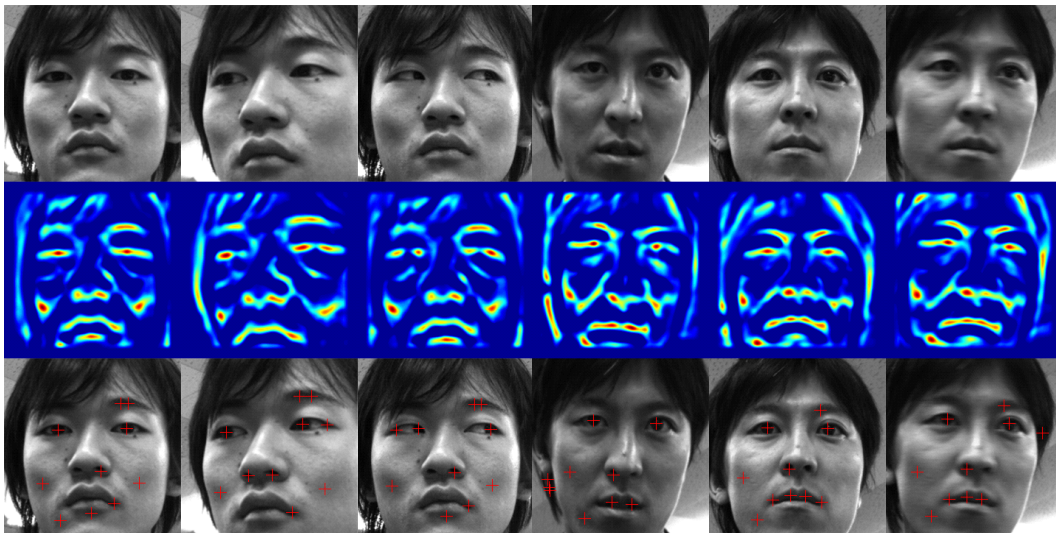


Figure 9. Top row: Input images, Middle row: Separability maps, Bottom row: Detection results

Filter type	Positioning errors (pixel)
CSF	1.101
SSF	1.636
Arithmetic mean	1.267
Geometric mean	1.313

Table 1. Averages of positioning error.

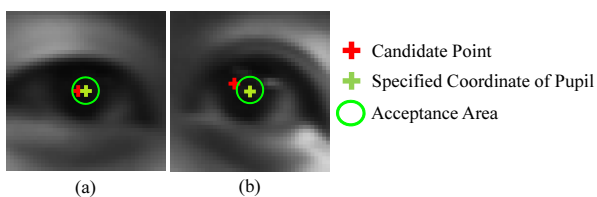


Figure 10. Experiment results. (a) An example of a success case: enlarged image of a part of the pupil, (b) An example of a failure case: enlarged image of a part of the pupil.

5 Conclusion

This paper has proposed a fast combined separability filter for detecting circular feature points. The proposed filter has achieved a processing speed seventy times faster than that of the conventional circular separability filter and high positioning accuracy at the same time by combining the outputs of four rectangle separability filters. The validity of the proposed filter has been shown clearly through the evaluation experiments with synthetic images and real face images.

6 Acknowledgment

This work was supported by KAKENHI (22300195).

References

- [1] G. Bradski. The OpenCV Library. *Dr. Dobb's Journal of Software Tools*, 2000.
- [2] K. Fukui. Edge extraction method based on separability of image features. *IEICE Transactions on Information and Systems*, E78(D(12)):1533–1538, 1995.
- [3] K. Fukui and O. Yamaguchi. Facial feature point extraction method based on combination of shape extraction and pattern matching. *Systems and Computers in Japan*, 29(6):49–58, 1998.
- [4] Y. Goshima and etc. Computational analysis of the effects of antineoplastic agents on axonal transport. *Journal of Pharmacological Sciences*, 114(2):168–179, 2010.
- [5] R. Lienhart and J. Maydt. An extended set of haar-like features for rapid object detection. *IEEE ICIP*, 1:900–903, 2002.
- [6] K. Mitsuhashi, H. Takemura, and H. Mizoguchi. Tracking control of sound spot around head using separability filter. *SICE Annual Conference*, pages 182–186, 2008.
- [7] O.A. randjelović and R. Cipolla. A pose-wise linear illumination manifold model for face recognition using video. *Computer Vision and Image Understanding*, 113(1):113–125, 2009.
- [8] F. Sakaue, T. Migita, T. Shakunaga, J. Satake, M. Chikaman, and H. Ueda. Face discrimination system for dialog interface robot in ubiquitous. *IEICE Technical Report PRMU2005-88 (in Japanese)*, pages 27–32, 2005.
- [9] T. Shimawaki, T. Sakiyama, J. Miura, and Y. Shirai. Estimation of ball route under overlapping with players and lines in soccer video image sequence. *International Conference on Pattern Recognition*, 1:359–362, 2006.
- [10] O. Yamaguchi, K. Fukui, and K. Maeda. Face recognition using temporal image sequence. *Proc. IEEE International Conference on Automatic Face and Gesture*, pages 318–323, 1998.